Title

The thermal decomposition of the benzyl radical in a heated micro-reactor. II. Pyrolysis of the tropyl radical

Journal

The Journal of Chemical Physics, 145(1)

ISSN

0021-9606

Authors

Buckingham, Grant T

Porterfield, Jessica P

Kostko, Oleg

et al.

Publication Date

2016-07-07

DOI

10.1063/1.4954895

Peer reviewed

The thermal decomposition of the benzyl radical in a heated micro-reactor. II. Pyrolysis of the tropyl radical

Grant T. Buckingham, Jessica P. Porterfield, Oleg Kostko, Tyler P. Troy, Musahid Ahmed, David J. Robichaud, Mark R. Nimlos, John W. Daily, and G. Barney Ellison

Citation: The Journal of Chemical Physics **145**, 014305 (2016); doi: 10.1063/1.4954895
View online: http://dx.doi.org/10.1063/1.4954895
View Table of Contents: http://scitation.aip.org/content/aip/journal/jcp/145/1?ver=pdfcov
Published by the AIP Publishing

The thermal decomposition of the benzyl radical in a heated micro-reactor. II. Pyrolysis of the tropyl radical

Grant T. Buckingham,[1,2] Jessica P. Porterfield,[1] Oleg Kostko,[3] Tyler P. Troy,[3] Musahid Ahmed,[3] David J. Robichaud,[2] Mark R. Nimlos,[2] John W. Daily,[4] and G. Barney Ellison[1]

[1]*Department of Chemistry and Biochemistry, University of Colorado, Boulder, Colorado 80309-0215, USA*
[2]*National Bioenergy Center, National Renewable Energy Laboratory, 15013 Denver West Parkway, Golden Colorado 80401, USA*
[3]*Chemical Sciences Division, Lawrence Berkeley National Laboratory, Berkeley, California 94720, USA*
[4]*Department of Mechanical Engineering, Center for Combustion and Environmental Research, University of Colorado, Boulder, Colorado 80309-0427, USA*

(Received 18 April 2016; accepted 15 June 2016; published online 5 July 2016)

Cycloheptatrienyl (tropyl) radical, C_7H_7, was cleanly produced in the gas-phase, entrained in He or Ne carrier gas, and subjected to a set of flash-pyrolysis micro-reactors. The pyrolysis products resulting from C_7H_7 were detected and identified by vacuum ultraviolet photoionization mass spectrometry. Complementary product identification was provided by infrared absorption spectroscopy. Pyrolysis pressures in the micro-reactor were roughly 200 Torr and residence times were approximately 100 μs. Thermal cracking of tropyl radical begins at 1100 K and the products from pyrolysis of C_7H_7 are only acetylene and cyclopentadienyl radicals. Tropyl radicals do not isomerize to benzyl radicals at reactor temperatures up to 1600 K. Heating samples of either cycloheptatriene or norbornadiene never produced tropyl (C_7H_7) radicals but rather only benzyl ($C_6H_5CH_2$). The thermal decomposition of benzyl radicals has been reconsidered without participation of tropyl radicals. There are at least three distinct pathways for pyrolysis of benzyl radical: the Benson fragmentation, the methyl-phenyl radical, and the bridgehead norbornadienyl radical. These three pathways account for the majority of the products detected following pyrolysis of all of the isotopomers: $C_6H_5CH_2$, $C_6H_5CD_2$, $C_6D_5CH_2$, and $C_6H_5{}^{13}CH_2$. Analysis of the temperature dependence for the pyrolysis of the isotopic species ($C_6H_5CD_2$, $C_6D_5CH_2$, and $C_6H_5{}^{13}CH_2$) suggests the Benson fragmentation and the norbornadienyl pathways open at reactor temperatures of 1300 K while the methyl-phenyl radical channel becomes active at slightly higher temperatures (1500 K). *Published by AIP Publishing.* [http://dx.doi.org/10.1063/1.4954895]

I. INTRODUCTION

Resonance stabilized radicals are important in combustion processes because they are precursors to soot formation.[1] Modern transportation fuels include a large fraction[2,3] of aromatics (benzene, toluene, xylenes, alkylbenzenes, and the like); see Fig. 3 of Ref. 4. Consequently, benzyl radicals ($C_6H_5CH_2$) are important intermediates in the high-temperature oxidation of these fuels. The pyrolysis of the benzyl radical has recently been examined[5–7] and evidence was found for several complex decomposition pathways. Fig. 1 is an overview[7] of the products that were detected following the pyrolysis of the $C_6H_5CH_2$ radical. A pathway for fragmentation of benzyl radical to fulvenallene and the fulvenallenyl radical was suggested[8] by Benson in 1986. An isomer of the benzyl radical is the cycloheptatrienyl (or tropyl) radical, C_7H_7. The relationship of tropyl to the benzyl radical is shown in Fig. 1. In the early literature, the interconversion of benzyl to tropyl ($C_6H_5CH_2 \leftrightharpoons C_7H_7$) was considered by several groups.[9–15] However, all recent theoretical studies[16–18] find no pathways below 2000 K for the isomerization of benzyl to tropyl. A photoionization search for the isomerization of the $C_6H_5CD_2$ benzyl radical to the $C_7H_5D_2$ tropyl radical with tunable VUV radiation found no evidence for tropyl radical formation.[7] To date, there are no experimental studies of the thermal decomposition of the tropyl radical, C_7H_7 (+ M) → products.

The focus of this paper is to generate authentic samples of the tropyl radical and to examine the pyrolysis pathways: C_7H_7 (+ M) → products. Earlier photoionization studies[19] of the C_7H_7 radical found bitropyl, C_7H_7—C_7H_7, to be a convenient thermal precursor for tropyl. As sources of tropyl radicals, we have investigated the flash-pyrolysis of bitropyl, cycloheptatriene, and norbornadiene. The hydrocarbon samples were diluted in a carrier gas of He or Ne and subjected to pyrolysis in a heated silicon carbide (SiC) micro-reactor. The micro-reactor was resistively heated to temperatures up to 1600 K and operated at pressures of roughly 200 Torr. Approximate residence times[20] in the reactor are 100 μs after which the gas mixture exits into a vacuum chamber at a pressure of 10^{-6} Torr. The resulting pyrolysis products are entrained in a molecular beam and are analyzed by a combination of photoionization mass spectroscopy (PIMS) and matrix infrared (IR) absorption spectroscopy.

Because of its importance in organic chemistry, atmospheric chemistry, and combustion processes, the benzyl

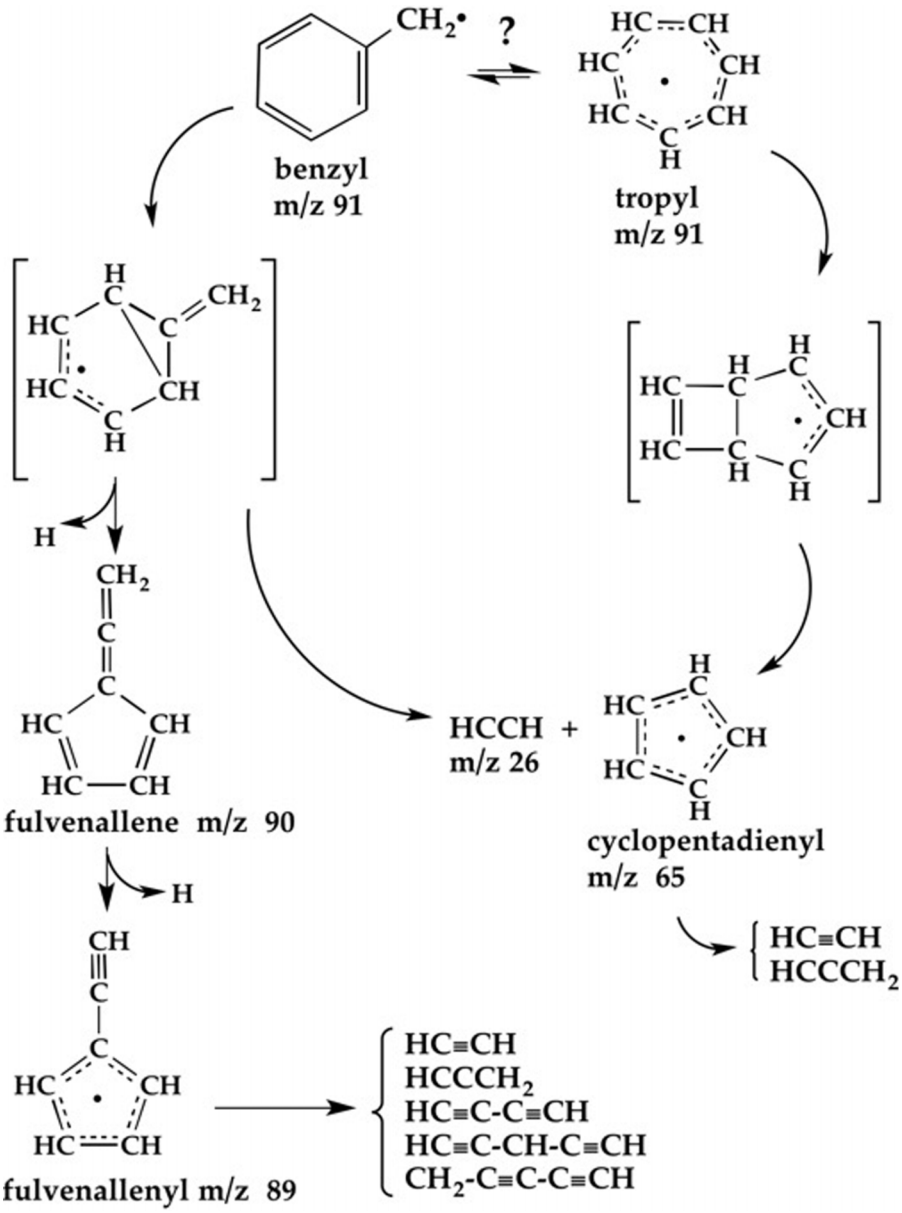

FIG. 1. The Benson pathway[8] for the pyrolysis of benzyl radical[7] is shown. A possible link of the $C_6H_5CH_2$ radical to the C_7H_7 radical is indicated.

radical ($C_6H_5CH_2$, $\tilde{X}\ ^2B_1$) has been extensively studied and a list of its properties is collected in Table 1 of Ref. 7. The tropyl radical (C_7H_7, $\tilde{X}\ ^2E_2''$) is not as well characterized experimentally. Because the tropyl radical has no electric dipole moment, there are no microwave spectra. To date, there are published laser induced fluorescence (LIF) spectra[11,12] of the tropyl radical, an IR-UV double resonance study with a free electron laser,[15] and preliminary helium nanodroplet IR absorption spectra.[21] There is no definitive analysis of the infrared spectrum of C_7H_7. Some of the available experimental properties of the tropyl radical are summarized in Table I.

This paper will demonstrate that pyrolysis of the tropyl radical only produces acetylene and the cyclopentadienyl radical. The tropyl radical does not isomerize to benzyl radical under any conditions observed in this work. As part of the final discussion, we will reconsider the thermal cracking of the $C_6H_5CH_2$ radical in the absence of C_7H_7. We present three separate pathways for the pyrolysis of the benzyl radical that seem to account for all of the current experimental findings, $C_6H_5CH_2$ (+ M) → products.

II. EXPERIMENTAL METHODS

A. Heated micro-reactor pyrolysis source

To carry out flash-pyrolysis of target molecules, we employ a resistively heated silicon carbide (SiC) reactor with an inner diameter (I.D.) of either 1.0 mm or 0.6 mm and a relatively short heated length, 10–15 mm. This geometry along with the present flow conditions allows[20] for short residence times of around 100 μs. At the exit of the reactor the gas is cooled as it expands into a vacuum chamber pumped to 10^{-4}–10^{-6} Torr, where reactive collisions cease. To monitor the temperature of the reactor, a type-C thermocouple is attached to the reactor's outer wall using tantalum wire as described previously.[22] The fluid mechanics of the heated micro-reactors were the subject of a recent detailed computational fluid dynamics investigation[20] that

TABLE I. Relevant experimental properties and ionization energies.

Tropyl and benzyl radical experimental properties	
$\Delta_f H_{298}(C_7H_8)$	43.2 ± 0.5 kcal mol^{-1} (181 ± 2 kJ mol^{-1})[71]
$\Delta_f H_{298}(C_7H_7\ \tilde{X}\ ^2E_2'')$	65.0 ± 0.7 kcal mol^{-1} (272 ± 3 kJ mol^{-1})[71]
$DH_{298}(C_7H_7$—H)	73.9 ± 0.5 kcal mol^{-1} (309 ± 2 kJ mol^{-1})[30]
$\Delta_f H_{298}(C_6H_5CH_3)$	12.0 ± 0.1 kcal mol^{-1} (50.4 ± 0.6 kJ mol^{-1})[71]
$\Delta_f H_{298}(C_6H_5CH_2\ \tilde{X}\ ^2B_1)$	49.6 ± 0.6 kcal mol^{-1} (208 ± 3 kJ mol^{-1})[71,72]
$DH_{298}(C_6H_5CH_2$—H)	89.8 ± 0.6 kcal mol^{-1} (376 ± 3 kJ mol^{-1})[71,72]
$\Delta_f H_{298}$(norbornadiene, C_7H_8)	58.8 ± 0.7 kcal mol^{-1} (246 ± 3 kJ mol^{-1})[71]
$\Delta_f H_{298}(C_5H_6)$ (cyclopentadiene)	32.1 ± 0.4 kcal mol^{-1} (134 ± 2 kJ mol^{-1})[71]
$\Delta_f H_{298}(C_5H_5,\ \tilde{X}\ ^2E_1'')$	63 ± 1 kcal mol^{-1} (264 ± 6 kJ mol^{-1})[73]
$DH_{298}(C_5H_5$—H)	83 ± 1 kcal mol^{-1} (348 ± 6 kJ mol^{-1})[71,73]
$DH_{298}(C_6H_5$—H)	112.9 ± 0.5 kcal mol^{-1} (472 ± 2 kJ mol^{-1})[71,72]
$\Delta_{rxn}H_{298}(C_7H_7 \rightarrow$ HCCH + C_5H_5)	53 ± 2 kcal mol^{-1} (220 ± 7 kJ mol^{-1})[7]
$AE(C_7H_8 \rightarrow C_7H_7^+ + H)$	9.36 ± 0.02 eV[30]
$\Delta_{isomeriz'n}H_{298}(C_6H_5CH_2\ \tilde{X}\ ^2B_1 \rightarrow C_7H_7\ \tilde{X}\ ^2E_2'')$	15.3 ± 0.9 kcal mol^{-1} (64 ± 4 kJ mol^{-1})[7]
Important ionization energies	
CH_3	9.8380 ± 0.0004 eV[74]
HC≡CH	11.400 81 ± 0.000 01 eV[75]
$HCCCH_2$	8.7006 ± 0.0002 eV[38]
CH_2CHCH_2	8.131 46 ± 0.000 25 eV[76,77]
o-C_6H_4	9.03 ± 0.05 eV[78]
$C_5H_5,\ \tilde{X}\ ^2E_1''$	8.4268 ± 0.0005 eV[35]
C_5H_4—C≡CH	8.19 ± 0.02 eV[79]
C_5H_4=C=CH_2	8.22 ± 0.01 eV[79]
$C_7H_7,\ \tilde{X}\ ^2E_2''$	6.221 ± 0.006 eV[9,19]
$C_6H_5CH_2,\ \tilde{X}\ ^2B_1$	7.2487 ± 0.0006 eV[77,80]
$C_6H_5CH_3$	8.8276 ± 0.0006 eV[81]
C_7H_8 (cycloheptatriene)	8.29 ± 0.01 eV[82]
C_7H_8 (2, 5 norbornadiene)	≤ 8.35 ± 0.01 eV[82]

modeled the pressure and temperature in the reactor at wall temperatures up to 1600 K. The findings in this study show that for a given set of reactor conditions and kinetic parameters, decomposition occurs within a small "sweet-spot" that can be as small as only a few mm of the total heated length. Another important finding was that the temperature, pressure, and thus decomposition rates can vary dramatically upon varying the experimental parameters, including: (1) carrier gas (argon, neon, and helium are all commonly used), (2) upstream and downstream pressure, and (3) mass flow rate, which can be controlled either by use of commercial mass flow controllers or with a pulsed valve. Therefore when comparing results from different experimental techniques, some variation is expected for the onset temperature of decomposition and/or the product ratios of competing decomposition pathways.

B. Photoionization mass spectroscopy

1. Pulsed VUV radiation

The 355 nm output light of a commercial Nd:YAG laser (Spectra Physics Pro-230-10) is focused into a tripling cell filled to 150 Torr with a 9:1 mixture of argon:xenon, which produces 118.2 nm (10.487 eV) photons. At the exit of the tripling cell is a MgF_2 lens used to focus the 118.2 nm light into the interaction region of the Jordan time-of-flight spectrometer. This tripling process has been well-studied[23] and has an efficiency[24,25] of around 1×10^{-5}. Additional losses are introduced by incomplete transmission of 118.2 nm light through the Mg_2F lens and intentional off-axis alignment through the lens to spatially separate 118.2 nm light from the remaining 355 nm light that exits the tripling cell, which can cause unwanted multiphoton ionization. As a result, laser powers of 10 mJ pulse^{-1} at 355 nm yield roughly 10 nJ pulse^{-1} of 118.2 nm. The region where the ionizing radiation and molecular beam are intersected is maintained at 10^{-7} Torr by a turbomolecular pump. Any molecule with ionization energy less than 10.487 eV is ionized and the resulting ions are accelerated into a reflectron time-of-flight spectrometer. In order to sustain sufficiently low pressure to maintain collisionless conditions, the gas flow must be pulsed with a Parker general valve operating at 10 Hz with 1 ms opening time. Backing pressures behind the pulsed valve are typically 2000 Torr of helium carrier gas and the pressure downstream of the reactor is typically 10^{-6} Torr, maintained by an 11-in. diffusion pump. Spectra shown in this work are the result of signal averaging of 1000 scans.

2. Continuous VUV radiation

A similar experimental setup for the micro-reactor scheme is used at the Chemical Dynamics Beamline endstation 9.0.2 at the advanced light source (ALS) in the Lawrence Berkeley National Laboratory. Using synchrotron light for PIMS adds a new experimental degree of freedom: tunable photon energy.[26] The energy of the synchrotron photons can be tuned between 7.4 eV and 30 eV, sufficiently high to ionize all species produced in the heated reactor. By measuring ion current at a single mass-to-charge ratio (m/z) while varying the photon energy and normalizing to the measured VUV power, it is possible to record photoionization spectra, which can be used to identify individual isomers that may be present. Signal averaging is used to increase signal-to-noise ratio; typical spectra are the composite of between 5×10^4 and 2×10^5 sweeps. To control the flow of gas through the reactor, an MKS mass flow controller is used along with a slightly smaller SiC reactor with an I.D. of 0.6 mm. Typical flow conditions include setting the flow controller to 200 standard cm^3 min^{-1} (sccm) backed by 5 atm of He. This yields pressures of 100 Torr between the mass flow controller and entrance of the reactor and roughly 10^{-4} Torr at the exit of the nozzle. With a 1 mm skimmer, the pressure in the ionization chamber can be maintained at roughly 5×10^{-6} Torr by a large turbomolecular pump.

C. Matrix isolation Fourier transform infrared spectroscopy

Since all polyatomic molecules possess characteristic vibrational spectra, IR spectroscopy is an excellent technique for identifying molecular species and serves as valuable complement to the PIMS experiments. The matrix IR spectrometer has been described before.[27,28] Briefly, a 1 mm I.D. SiC reactor is coupled to a pulsed valve assembly very

similar to the PIMS system described above. The upstream pressure is between 800 and 1000 Torr, and with the pulsed valve operating with a roughly 1 ms opening time and 15 Hz repetition rate, the pressure at the reactor exit is typically 10^{-6} Torr, which is maintained with a small turbomolecular pump. The output of the reactor impinges on a cryogenically cooled CsI window 4 cm downstream that is maintained at 5 K by a helium cryostat. The carrier gas for this experiment is neon, which condenses into a solid matrix upon colliding with the 5 K window. A standard matrix is formed by flowing 200 Torr of sample mixture from a roughly 3 liter gas manifold, which leads to a deposition time of around 1 h. After dosing is complete, the reactor assembly is rotated 90° out of the way and the CsI window is lowered into the beampath of a commercial Fourier transform IR spectrometer (Nicolet 6700). The MCT-A detector has a spectral range of 4000–600 cm^{-1} and is operated with 0.25 cm^{-1} resolution, with typical spectra constructed by averaging 500 scans. Although the neon matrix is chemically inert, it does affect the vibrational spectra of entrained molecules. Average matrix shifts are on the order of 1–5 cm^{-1} from the unperturbed, gas-phase values.

D. Sample preparation

Pyrolysis of bitropyl (7,7′-bi(1,3,5-cycloheptatriene)) is a good source of the tropyl radical.[19] Cleavage of the C—C bond produces two tropyl radicals,

$$C_7H_7—C_7H_7(+M) \rightarrow C_7H_7 + C_7H_7. \quad (1)$$

The bond energy, DH_{298} (C_7H_7—C_7H_7), was measured[29] to be 43 ± 1 kcal mol^{-1}. Bitropyl is solid at room temperature and was purchased from Sigma-Aldrich and used without further purification. Another tropyl precursor, cycloheptatriene (C_7H_8), was explored. The C—H bond strength[30] of cycloheptatriene is 74 kcal mol^{-1} and this implies that C_7H_8 could be an attractive thermal precursor for the tropyl radical; see Table I. Cycloheptatriene is a liquid at room temperature and was purchased from Sigma-Aldrich with a purity of 95% and used without further purification. A final potential precursor for tropyl radical to be considered is 2,5-norbornadiene. This hydrocarbon was purchased from Sigma-Aldrich with 98% purity and was used without further purification. All of the pyrolysis experiments use dilute gas samples with either helium or neon as the carrier gas. Previous work with SiC reactors[7,31,32] has shown that bimolecular chemistry can obscure decomposition spectra so samples were made as dilute as possible while maintaining sufficient signal-to-noise. Typical dilutions are 0.1%–0.01%. For some experiments the dilution is difficult to control because the solid bitropyl precursor must be heated to 50–65 °C to achieve sufficient vapor pressure, depending on the gas flow rate and amount of sample surface area present. At the ALS, the sample was heated in a 1 cm I.D. glass test tube and He carrier gas was directed over the surface before traveling downstream to the reactor. The matrix IR experiments make use of a 1 mm I.D. glass vial that is inserted directly behind the pulse valve, where it is then heated. Pyrolysis appears to be unimolecular since no change in products was observed over a range of sample temperatures.

III. RESULTS AND DISCUSSION

Fig. 2 shows the 9.5 eV PIMS spectrum that results from a dilute sample of bitropyl being heated in a continuous flow micro-reactor to 600 K, where there should be no thermal decomposition of bitropyl. Earlier threshold photoelectron spectra of bitropyl reported[19] ions at both m/z 91 and 182 with VUV photons of 8.7 eV. The 9.5 eV spectrum in Fig. 2 shows signals at m/z 91 and 104 only; there are no parent ions at m/z 182 indicating that the bitropyl sample is completely dissociatively ionized,

$$C_7H_7—C_7H_7 + 9.5 \text{ eV} \rightarrow [C_7H_7—C_7H_7]^+ \rightarrow \text{products}. \quad (2)$$

The m/z 91 ion is $C_7H_7^+$ while the smaller feature at m/z 104 remains unidentified but given its similar response to heating as other dissociative ionization products, we believe it is not a contaminant but rather that it stems from dissociative ionization of bitropyl. The results in Fig. 2 are consistent with earlier PIMS studies,[29] which revealed that the appearance energy for the $C_7H_7^+$ ion from bitropyl was 8.09 ± 0.05 eV. The extensive dissociative ionization in Fig. 2 results from the fragmentation of the $[C_7H_7—C_7H_7]^+$ cation into a pair of exceptionally stable products: $\tilde{X}\ ^2E_2''C_7H_7$ and $\tilde{X}\ ^{+1}A_1'\ C_7H_7^+$, which is an aromatic cation.

Fig. 3 shows the PIMS spectra that result as bitropyl is heated in the micro-reactor up to 1500 K. As the sample is heated to 1100 K, the 11.8 eV PIMS reveals the appearance of a peak at m/z 26 (circled in red) that is shown to be $HCCH^+$ by PIE spectra. The signal at m/z 65 is assigned to $C_5H_5^+$ via PIE spectra at reactor temperatures of 1200 K and higher. At temperatures below 1100 K, signals at m/z

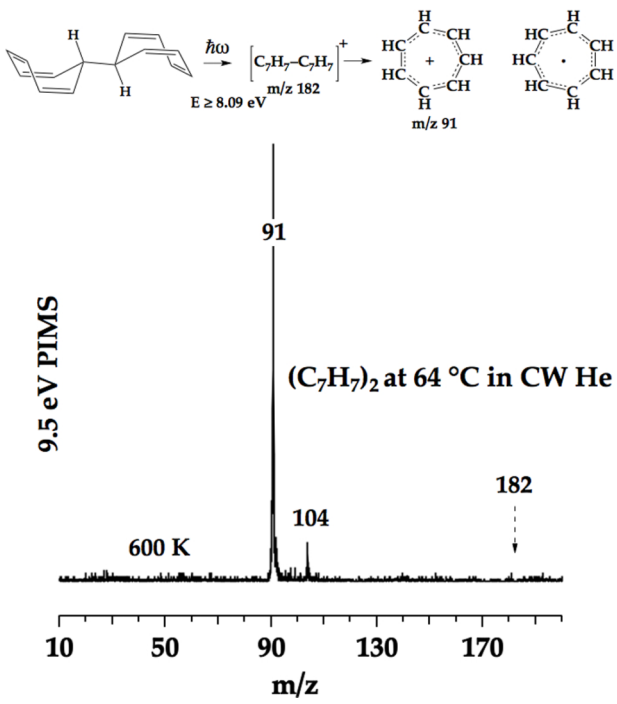

FIG. 2. The 9.5 eV PIMS spectra of bitropyl (C_7H_7—C_7H_7 m/z 182) pyrolyzed in a continuous flow micro-reactor heated to 600 K. The absence of a signal at m/z 182 indicates that the bitropyl sample is dissociatively ionized. The feature at 104 is the result of dissociative ionization of the precursor and is probably $[styrene]^+$.

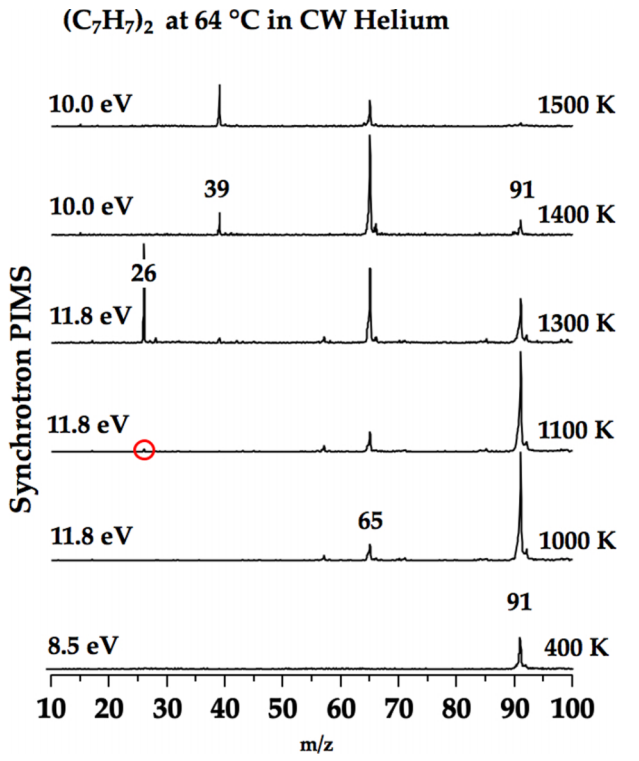

FIG. 3. PIMS spectra of bitropyl (C_7H_7—C_7H_7) recorded in a continuous flow micro-reactor at temperatures of 400 K, 1100 K, 1200 K, 1300 K, 1400 K, and 1500 K. Pyrolysis of tropyl (C_7H_7 (+ M) → HCCH + C_5H_5) commences at 1100 K as indicated by the small signal for $HCCH^+$ at m/z 26 (denoted with a red circle).

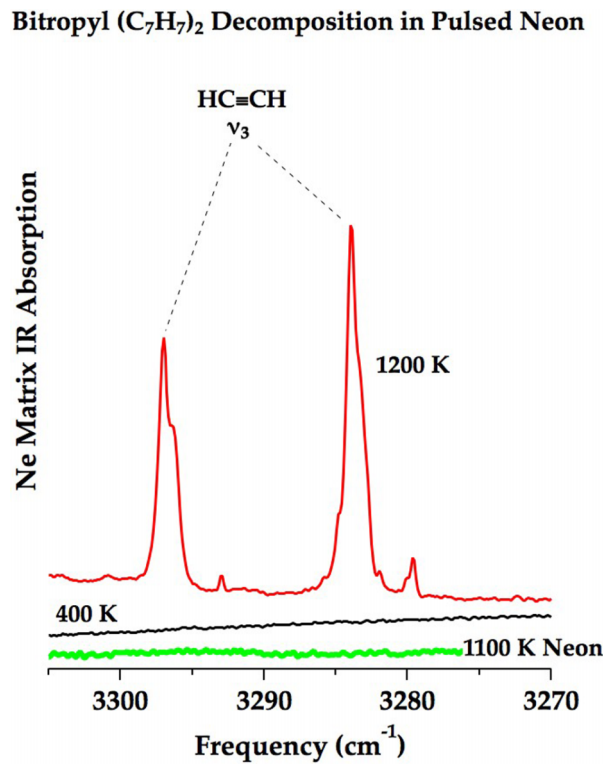

FIG. 5. Neon matrix absorption IR spectrum of the 1200 K pyrolysis of bitropyl (C_7H_7—C_7H_7) in a pulsed micro-reactor is shown in red. The presence of acetylene[83] is demonstrated by observation of the intense bands of ν_3(HCCH). The black trace is that of the bitropyl precursor, which is un-pyrolyzed at 400 K. The green trace is the background spectrum of pure Ne heated to 1100 K.

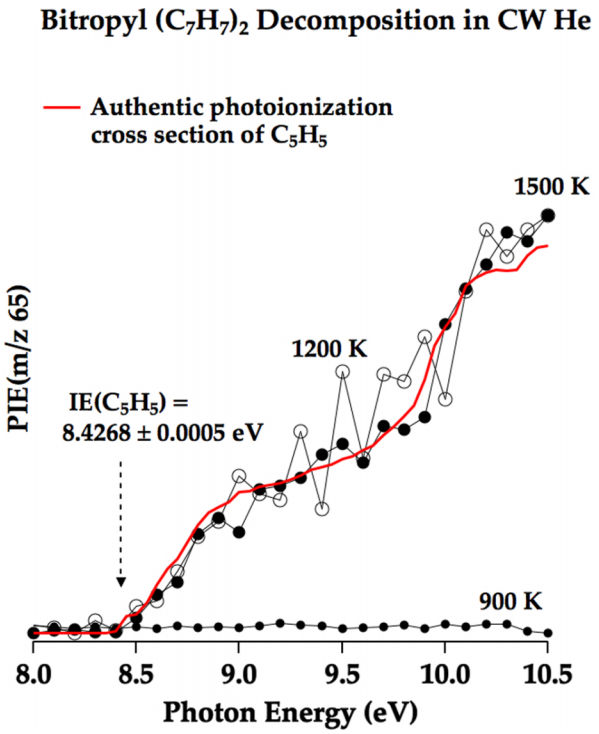

FIG. 4. PIE (m/z 65) recorded during the thermal decomposition of bitropyl (C_7H_7—C_7H_7) in a continuous flow micro-reactor in He at 900 K, 1200 K, and 1500 K. The red trace is the PIE spectrum of the C_5H_5 radical recorded previously.[36] The ionization threshold[35] for $\tilde{X}\ ^2E_1''$ C_5H_5 is indicated. There is no evidence for cyclopentadienyl radical being present at 900 K.

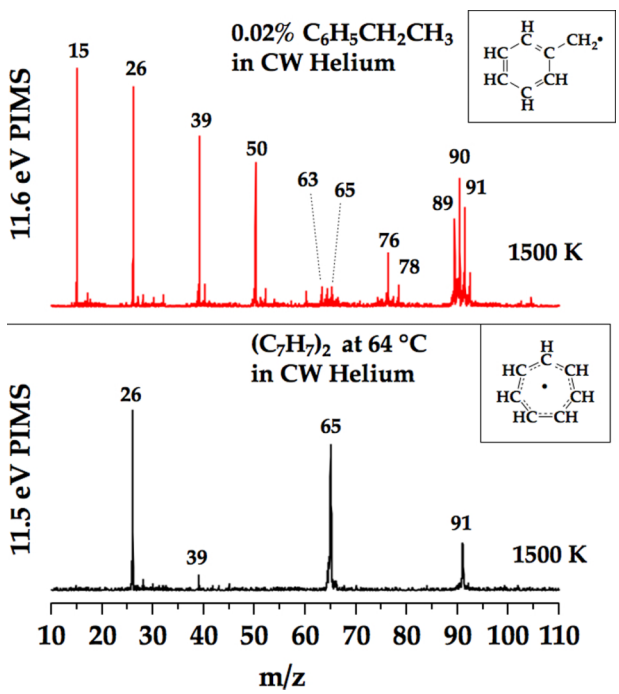

FIG. 6. PIMS spectra comparing the thermal decomposition of the benzyl radical and the tropyl radical. In both experiments the precursors (ethyl benzene and bitropyl) are decomposed in a continuous, 0.6 mm I.D. micro-reactor that is heated to 1500 K. No isomerization from the C_7H_7 radical to the more stable $C_6H_5CH_2$ is observed, as indicated by the paucity of benzyl decomposition products found in tropyl decomposition spectra.

65 arise from dissociative ionization. Since the ionization energy of acetylene is so large (11.4 eV, see Table I), the signal at m/z 26 will only arise from photoionization of thermally produced HC≡CH and not from dissociative ionization. When molecules are ionized with excess photon energy, cations are formed with internal energy that can be used to fragment the cation to a daughter ion and a neutral fragment(s). Dissociative ionization pathways are generally governed by energetic considerations. A pathway that produces $HCCH^+$ and C_5H_5 will be energetically less favorable than one producing $HCCH + C_5H_5^+$ by 3 eV, given the difference in ionization energies (IE(HCCH) = 11.4 eV and IE(C_5H_5) = 8.4 eV). By recording PIMS at 11.8 eV, we conclude that the feature at m/z 65 results from dissociative ionization whenever the co-produced fragment, HC≡CH, is not detected. At 1100 K and hotter, the spectra imply thermal cracking of tropyl to acetylene and cyclopentadienyl,

$$C_7H_7\ \tilde{X}\ ^2E_2''(+M) \rightarrow HC{\equiv}CH + C_5H_5\ \tilde{X}\ ^2E_1''. \qquad (3)$$

As the reactor temperature is increased to 1500 K, the pyrolysis of tropyl radical is complete and m/z 91 is no longer present. At 1400 K, a 10.0 eV PIMS signal at m/z 39 is detected that is assigned to propargyl radical; the IE($HCCCH_2$) is 8.7 eV (see Table I). In earlier studies,[7,33,34] it was observed that at 1300 K the cyclopentadienyl radical thermally dissociates to propargyl radical and acetylene,

$$C_5H_5(+M) \rightarrow HC{\equiv}CH + HCCCH_2. \qquad (4)$$

The thermal decomposition of the tropyl radical from 1200 K up to 1500 K is remarkably simple. We observe features at m/z 65 and 26 that are predicted to be cyclopentadienyl and acetylene, consistent with Eq. (3) and Fig. 1. To confirm the identity of the feature at m/z 65, the PIE spectrum of m/z 65 was recorded between 8.0 and 10.5 eV; see Fig. 4. At 900 K and below there is no signal for PIE(m/z 65). At temperatures of 1200 K and above, the PIE for m/z 65 shows a threshold at 8.5 ± 0.1 eV, consistent with the observed[35] IE(C_5H_5) of 8.4 eV (see Table I). The PIE(m/z 65) at 1200 K and 1500 K in Fig. 4 agrees with the PIE of an authentic sample[36] of C_5H_5. The assignment of m/z 39 to the propargyl radical in Fig. 3 is also confirmed[37] by a measurement of the PIE(m/z 39). Both the threshold and the shape of the PIE(m/z 39) match the known[38] IE($HCCCH_2$) and photoionization cross section[39] of the propargyl radical.

Fig. 5 shows the neon matrix IR spectrum of the products of the thermal decomposition of bitropyl in a pulsed reactor at 1200 K. This vibrational spectrum confirms HC≡CH as a pyrolysis product of tropyl radical. Both the PIE(m/z 65) spectrum in Fig. 4 and the IR spectrum in Fig. 5 confirm the products in Eq. (3).

Fig. 6 is a contrast between the pyrolysis products of ethylbenzene (top) and bitropyl (bottom). Both samples are thermally decomposed in a 0.6 mm I.D., continuous flow

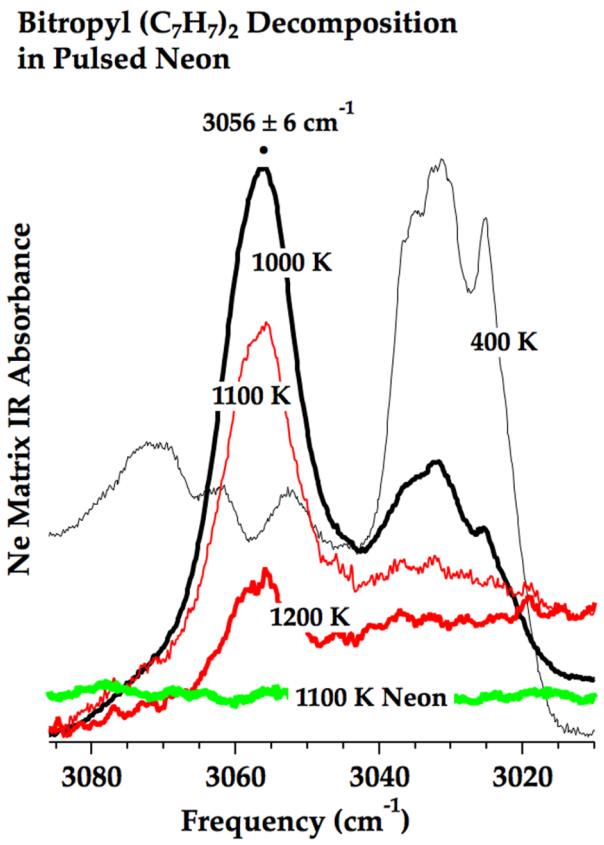

FIG. 7. Neon matrix absorbance IR spectra of the pyrolysis of bitropyl (C_7H_7—C_7H_7) in a pulsed micro-reactor at 400 K (thin black), 1000 K (thick black), 1100 K (thin red), and 1200 K (thick red). The feature at 3030 cm^{-1} is assigned as the bitropyl precursor. A new band at 3056 ± 6 cm^{-1} is assigned to the C_7H_7 radical. This assignment is corroborated by the temperature dependence observed here and in the PIMS of Fig. 3. The green trace is a background spectrum of Ne heated to 1100 K.

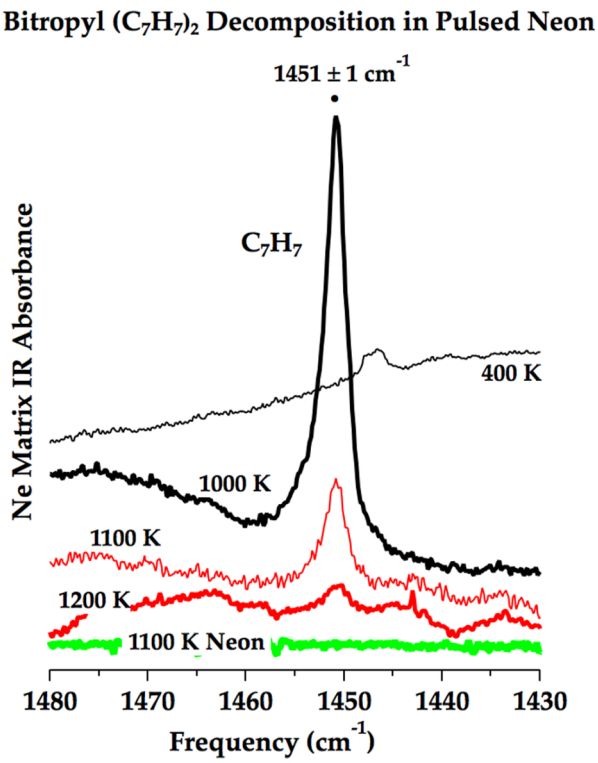

FIG. 8. Neon matrix absorbance IR spectra of the pyrolysis of bitropyl at 400 K (thin black), 1000 K (thick black), 1100 K (thin red), and 1200 K (thick red). The absorption feature at 1451 ± 1 cm^{-1} is assigned to the tropyl radical. The green scan is a background spectrum of Ne heated to 1100 K.

micro-reactor that is heated to 1500 K. The thermal cracking of $C_6H_5CH_2CH_3$ initially generates[7] methyl radicals (m/z 15) and benzyl radicals (m/z 91). Subsequent fragmentation of the $C_6H_5CH_2$ radical leads to the complex set of products at m/z 26, 39, 50, 63, 65, 76, 78, 89, and 90 that are discussed in Ref. 7. Pyrolysis of bitropyl at the bottom of Fig. 6 produces C_7H_7 (m/z 91) and the fragmentation products from tropyl, C_5H_5 (m/z 65), and HC≡CH (m/z 26). Propargyl radical, $HCCCH_2$ (m/z 39), results from the thermal cracking of the cyclopentadienyl radical, Eq. (4). The dramatic differences between these two PIMS spectra in Fig. 6 provide strong evidence that the tropyl radical does not isomerize to the benzyl radical.

A. Matrix isolation spectroscopy

Because of the extensive dissociative ionization of the tropyl radical precursor, C_7H_7—C_7H_7, the application of PIMS to study tropyl radical pyrolysis is somewhat limited. Photoions of the pyrolysis products will always be partially obscured by fragments of dissociative ionization. Consequently IR spectroscopy is a very useful complementary detection tool.

However, the matrix IR spectroscopy of tropyl radical has its own set of complications. There are no definitive vibrational spectra of the C_7H_7 radical in a matrix environment. The gas phase IR spectrum was recorded for the tropyl radical (formed in a discharge from cycloheptatriene) with an IR-UV double resonance technique[15] that used the free electron laser "FELIX." Several vibrational modes of tropyl were observed in the fingerprint region but none could be assigned. LIF spectroscopy[12] has been used to identify some of the modes of C_7H_7, $\tilde{X}\ ^2E_2''$. This study presented a vibrational analysis of the $\tilde{A}\ ^2E_3'' \leftarrow \tilde{X}$ electronic spectrum and several gas phase modes of the ground $^2E_2''$ state were reported. Unfortunately, because of the nature of LIF spectroscopy, there is no information available regarding IR intensities for the ground state C_7H_7, $\tilde{X}\ ^2E_2''$ fundamentals. An important complication for studying tropyl radical in a neon matrix is the presence of the Jahn–Teller effect, which distorts the tropyl radical from the D_{7h} surface to the C_{2v} surface. The effect of inert gas matrices on Jahn-Teller distorted molecules is not easy to predict and is expected to cause greater perturbations from gas-phase frequencies.

In spite of these difficulties, matrix isolation IR spectroscopy is useful as a secondary confirmation for tropyl radical decomposition. The precursor used is bitropyl and the experiments were performed using neon as the carrier gas. Fig. 7 shows four scans taken at different reactor temperatures for bitropyl decomposition: 400 K, 1000 K, 1100 K, and 1200 K; as well as a scan of pure neon run at 1100 K as a control to rule out any systematic contaminants. The thin black trace shows an absorption feature from the precursor, which has not undergone decomposition at 400 K. This peak is significantly depleted upon heating to 1000 K (thick black line) and a strong, broad feature has developed centered at $3056 \pm 6\ cm^{-1}$. Upon heating to 1100 K (thin red trace) and 1200 K (thick red trace), this new peak is depleted as tropyl radical thermally decomposes. The feature from the bitropyl precursor is completely absent by 1100 K. This temperature dependence is in qualitative agreement with that observed in Fig. 3, although one could expect minor discrepancies due to differing carrier gas (Ne vs. He) and flow conditions (pulsed vs. continuous). None of the vibrational features for tropyl radical in the CH stretch region have been previously assigned. A recent helium nanodroplet[21] study observed a pair of vibrational bands at $3052.9\ cm^{-1}$ and $3057.4\ cm^{-1}$ that are assigned to the tropyl radical. The helium nanodroplet spectra agree well with the matrix IR feature illustrated in Fig. 7. Fig. 8 shows an additional intense absorption feature appearing in the decomposition of bitropyl at $1451\ cm^{-1}$. This feature exhibits similar temperature dependence to that shown in Fig. 7; it is not observed at 400 K and is strongest at 1000 K and begins to decay at 1100 K and 1200 K.

Neither the $3056\ cm^{-1}$ nor the $1451\ cm^{-1}$ bands were observed in the spectra from benzyl decomposition[7] nor were any vibrational assignments for benzyl radical observed in the tropyl radical decomposition spectra. This provides further confirmation that the benzyl and tropyl radicals do not interconvert, even at temperatures where both radicals thermally decompose.

B. Cycloheptatriene or norbornadiene as tropyl precursors?

In addition to bitropyl, cycloheptatriene (C_7H_8) was considered as a pyrolytic source of C_7H_7. Cycloheptatriene has been successfully used as a precursor to prepare gas-

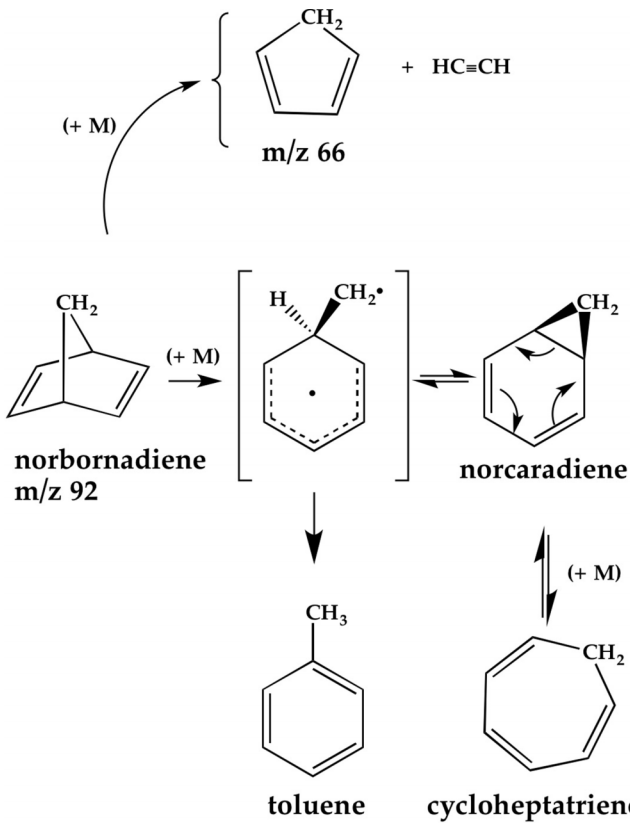

FIG. 9. Isomerizations[40–43] of norbornadiene, norcaradiene, cycloheptatriene, and toluene.

phase tropyl radicals in discharge sources.[10,12,15] However, shock tube studies[40] of high-temperature pyrolysis of cycloheptatriene demonstrate complete conversion of C_7H_8 to $C_6H_5CH_3$. A gas-phase, stirred-flow reactor was used[41] to explore the isomerizations of norbornadiene, cycloheptatriene, and toluene. No intermediate radicals could be detected in this early study because the reaction products were detected by gas chromatography with flame ionization detection. Fig. 9 is a summary[42] of the interconversions of norbornadiene, cycloheptatriene, and toluene. Norcaradiene[43] has been predicted as an intermediate in the equilibration of norbornadiene and cycloheptatriene. The first decomposition pathway of norbornadiene is the retro-Diels-Alder fragmentation to cyclopentadiene and acetylene. At higher temperatures, norbornadiene, norcaradiene, cycloheptatriene, and toluene all interconvert, where toluene is the most stable isomer.[41]

Fig. 10 shows the IR spectra of a dilute mixture of 0.05% cycloheptatriene in neon that was thermally decomposed in a pulsed micro-reactor. As predicted,[40] C_7H_8 isomerizes to toluene rather than forming tropyl radical. This finding was confirmed by assigning 11 absorption features to gas-phase[44] $C_6H_5CH_3$. At 300 K the only feature in this spectral window is due to the precursor, cycloheptatriene, but upon heating, three new bands emerge. The three peaks are assigned[44] as ν_{11} at 730 cm^{-1}, ν_4 at 695 cm^{-1}, and ν_{18b} at 1083 cm^{-1}, which agree well with the gas-phase values: ν_{11} = 728 cm^{-1}, ν_4 = 695 cm^{-1}, and ν_{18b} = 1080 cm^{-1}. At the highest temperature (1500 K), a few small features are observed that are assigned to $C_6H_5CH_2$ including ν_7 (762 cm^{-1}) and ν_{13} (1308 cm^{-1}), in agreement with the argon matrix spectrum of benzyl radical.[45]

The isomerization of C_7H_8 to $C_6H_5CH_3$ is confirmed by the 118.2 nm PIMS, shown in Fig. 11. In this experiment, cycloheptatriene is subjected to pyrolysis in a pulsed micro-reactor heated to 300 K, 1400 K, and 1600 K. The products shown at 1600 K are nearly identical to those observed from benzyl radical precursors[7] but with a higher temperature for decomposition onset; compare with top panel of Fig. 6.

We also studied the decomposition of 2,5-norbornadiene (Fig. 12). The IE(2,5-norbornadiene) is less than 8.35 eV (Table I) and the initial scan (400 K) reveals a small amount of dissociative ionization: norbornadiene + 118.2 nm → $C_6H_5CH_2^+$ (m/z 91) + H atom. At 1300 K, it is observed that norbornadiene undergoes a retro-Diels-Alder reaction: norbornadiene (+ M) → C_5H_6 (m/z 66) + HC≡CH (see Fig. 9). As the reactor is heated to 1600 K, it appears that 2,5-norbornadiene isomerizes to $C_6H_5CH_3$, which thermally dissociates to H atom and benzyl radical. The fragmentation of $C_6H_5CH_2$ (top scan in Fig. 12) is very similar to the pyrolysis pattern observed for norbornadiene (bottom Fig. 12). At higher reactor temperatures, the retro-Diels-Alder pathway is still active but is obscured by fragmentation of the product cyclopentadiene: C_5H_6 (+ M) → C_5H_5 (m/z 65) + H. See Fig. 5 of Ref. 46.

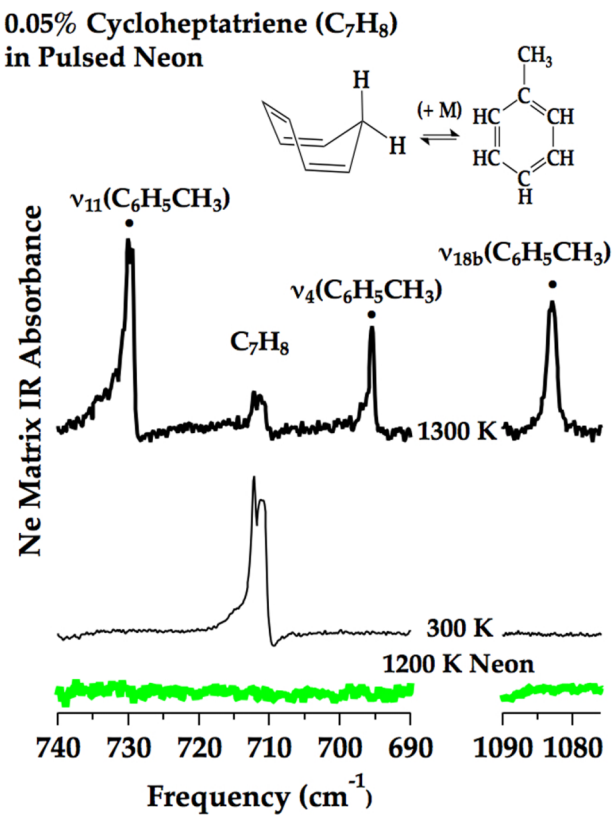

FIG. 10. The neon matrix absorbance IR spectrum of cycloheptatriene (C_7H_8) pyrolysis in a pulsed micro-reactor at 1300 K is shown in thick black. The thin black line is the absorbance spectrum of cycloheptatriene at 300 K. The 300 K spectrum shows only one feature belonging to C_7H_8. Upon heating to 1300 K, the precursor feature has diminished and new bands are observed. All three are assigned as vibrations of toluene[45]

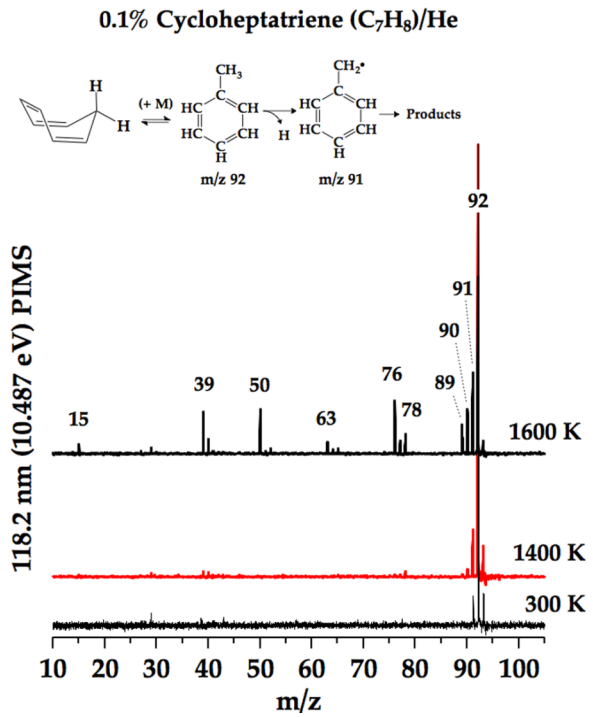

FIG. 11. PIMS spectra from the pyrolysis of cycloheptatriene in pulsed helium are shown at three reactor temperatures, 300 K, 1400 K, and 1600 K. At 1400 K the expected fragmentation of tropyl radical (see Fig. 3) is not observed. At 1600 K a set of products appears that is very similar to those characteristic[7] of benzyl radical decomposition (see Fig. 6).

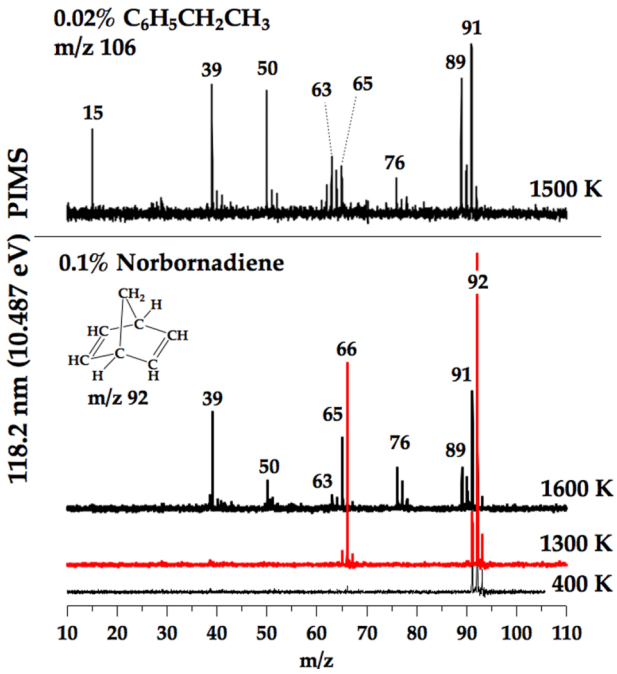

FIG. 12. PIMS spectra from the pyrolysis of norbornadiene in pulsed helium are shown at three reactor temperatures, 400 K, 1300 K, and 1600 K. At 1300 K norbornadiene undergoes a retro-Diels-Alder fragmentation and produces HCCH and C_5H_6 (m/z 66); bottom scan. At 1600 K a set of products appears that is very similar to those characteristics[7] of benzyl radical decomposition; top scan uses $C_6H_6CH_2CH_3$ as a source of benzyl radical.

IV. CONCLUSIONS

The results of Figs. 3–8 eliminate any participation of the C_7H_7 radical from the pyrolysis pathways of the $C_6H_5CH_2$ radical at temperatures up to 1600 K. Tropyl radical only decomposes to acetylene and the cyclopentadienyl radical, Eq. (3). These findings are consistent with the failure[7] of tunable PIMS to detect C_7H_7 radicals as benzyl undergoes pyrolysis. Very recently, time-resolved PIMS spectroscopy was used[47] to study soot formation. The addition of acetylene to propargyl radical in a slow flow quartz reactor at (10 Torr/1000 K) was found to induce molecular weight growth via the sequence: $HC{\equiv}CH + HCCCH_2 \rightarrow C_5H_5 \rightarrow C_7H_7$. This is exactly the reverse of the pyrolysis reactions (3) and (4) above. We conclude this paper with a reconsideration of the pathways for the thermal fragmentation of benzyl radical based on all experimental findings.[7,8,13,48–53]

The pyrolysis of the benzyl radical is a complex problem. None of the early experimental papers[53–58] describing the pyrolysis of $C_6H_5CH_2$ were able to identify any of the thermal fragments except for the H atoms detected by ARAS.[8,13] The only organic radicals resulting from pyrolysis of benzyl radical come from a few studies using heated micro-reactors outfitted with VUV PIMS.[5–7]

The pyrolysis of toluene was studied[5] in a quartz flow tube reactor at pressures of 8–15 Torr and temperatures of 1136–1507 K. A more recent study[6] of toluene pyrolysis used a heated alumina (Al_2O_3) micro-reactor coupled to a VUV PIMS driven by tunable radiation from a synchrotron. The 248 nm photochemistry of benzyl radical has been studied[59] by photofragment translational spectroscopy. Dissociation occurs following relaxation from the excited state[60] to the ground state, $C_6H_5CH_2$, $\tilde{X}\ ^2B_1$, producing benzyl radicals $(C_6H_5CH_2)^*$ excited by 5 eV. The benzyl* radicals fragment to H + C_7H_6 and CH_3 + C_6H_4 radicals.

As mentioned in the Introduction, pyrolysis of either ethylbenzene or benzyl bromide in a heated SiC micro-reactor[7] revealed an extended set of products that are summarized in Fig. 1. When $C_6H_5{}^{13}CH_2CH_3$ was heated[7] to 1200 K, the labeled benzyl radical, $C_6H_5{}^{13}CH_2$, was produced. Decomposition of $C_6H_5{}^{13}CH_2$ at 1300 K produced a mixture of ^{12}cyclopentadienyl and ^{13}cyclopentadienyl radicals. One pathway to incorporate the ^{13}C label into the cyclopentadienyl radical would be isomerization of $C_6H_5{}^{13}CH_2$ to ^{13}C-labeled C_7H_7 (see Fig. 1). However, the use[7] of 6.5 eV photons to search for the isomerization $C_6H_5CD_2 \rightarrow C_7H_5D_2$ detected no tropyl radicals. This failure to observe C_7H_7 radicals did not conclusively prove that tropyl is not present during the thermal cracking of benzyl radical. However, the current results in Figs. 3–8 demonstrate that clean samples of C_7H_7 radicals can be generated and that they fragment by a pathway independent of benzyl.

A. Pyrolysis of benzyl radical without tropyl

In all the pyrolysis experiments performed on benzyl radicals[7] or tropyl radicals (this paper), care was taken to study dilute samples (0.1%–0.02% hydrocarbons in He or Ne). In the analysis of these results, we assume all fragmentation products result from unimolecular chemistry; there is no bimolecular chemistry to be analyzed. Pathways for the unimolecular, thermal decomposition of the benzyl radical are shown in Figs. 13 and 14. These schemes are based on the experimental findings from shock tubes with ARAS detection[8,13] and heated micro-reactors monitored by PIMS and IR spectroscopy.[7] Heating the $C_6H_5CH_2$ radical to 1300 K triggers an "extended" Benson fragmentation. The original suggestion[8] only offered pathways for H atom loss and formation of the fulvenallenyl radical, C_5H_4—C≡CH. This mechanism[8] also implies formation of the cyclopentadienyl radical and acetylene. The bicyclic radicals and vinylidene[61,62] (:C=CH_2) in Fig. 13 will not be stable in the hot micro-reactor and are enclosed in brackets. The production of H atoms is known from both[8,13] ARAS and PIMS spectra.[7]

The Benson fragmentation in Fig. 13 leads to formation of the cyclopentadienyl and the fulvenallenyl radicals (one could view C_5H_4—C≡CH as a substituted cyclopentadienyl radical). As shown in Eq. (4), C_5H_5 decomposes to acetylene and propargyl radicals at 1300 K. Likewise the fulvenallenyl radical has been observed[63,64] to decompose to propargyl radical and diacetylene. This can be summarized,[37]

$$C_5H_4{-}C{\equiv}CH(+\,M) \rightarrow HCCCH_2 + HC{\equiv}C{-}C{\equiv}CH, \quad (5a)$$

$$C_5H_4{-}C{\equiv}CH(+\,M) \rightarrow HC{\equiv}CH + HC{\equiv}C{-}CH{-}C{\equiv}CH, \quad (5b)$$

$$C_5H_4{-}C{\equiv}CH(+\,M) \rightarrow HC{\equiv}CH + HC{\equiv}C{-}C{\equiv}C{-}CH_2. \quad (5c)$$

The presence of the cyclopentadienyl radical and HC≡CH is confirmed by PIMS, PIE, and IR spectroscopy.[7] PIMS and PIE spectroscopy also detect both C_5H_4=C=CH_2 and C_5H_4—C≡CH. The presence of fulvenallene is additionally confirmed by IR spectroscopy. PIMS and IR spectroscopy clearly identify the propargyl radical, $HCCCH_2$. PIMS signals at m/z 50 and 63 are consistent with the presence of HC≡C—C≡CH and the two radicals, CH_2—C≡C—C≡CH and HC≡C—CH—C≡CH. However, neither the PIE nor IR spectra could distinguish between the (CH_2—C≡C—C≡CH, HC≡C—CH—C≡CH) pair.

The Benson fragmentation predicts loss of H atom from $C_6H_5CH_2$ to produce a pair of isomers, C_5H_4=C=CH_2 and C_5H_5—C≡CH, both at m/z 90. Recently pyrolysis of $C_6H_5CD_2$ in a shock tube with ARAS detection[13] revealed the formation of both H and D atoms in agreement with this prediction. Pyrolysis of $C_6H_5CD_2CD_3$ in a micro-reactor[7] provided further support with the detection of both C_5H_4=C=CD_2 (m/z 92) and C_5H_5—C≡CD (m/z 91).

The Benson fragmentation shown in Fig. 13 cannot be the complete story for the thermal cracking of the benzyl radical. PIMS and PIE spectra confirm[7] that heating $C_6H_5{}^{13}CH_2$ radicals to 1300 K produces $^{13}CH_3$, ^{13}C-labeled C_5H_5, and *o*-C_6H_4; these products cannot be explained by Benson's mechanism.[8] Fig. 14 shows two additional pathways

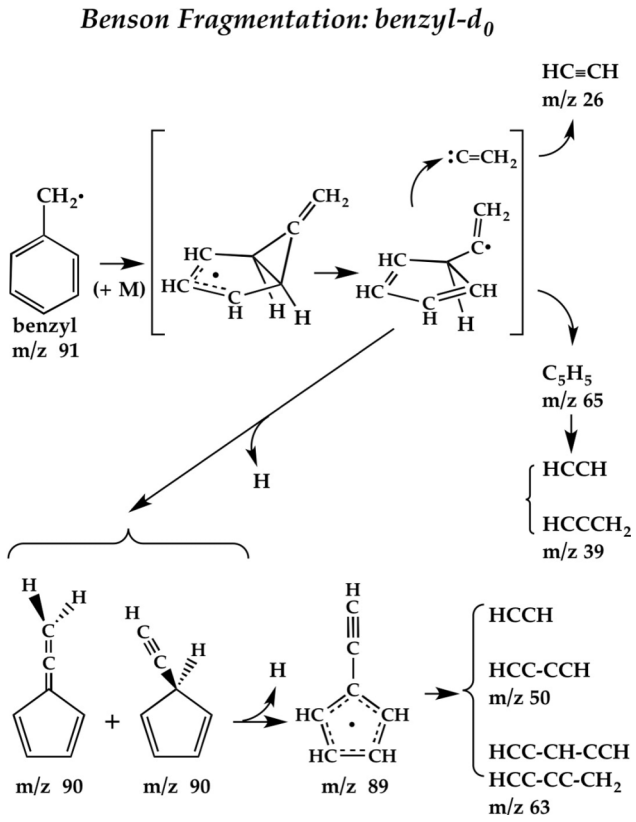

FIG. 13. The "extended" Benson fragmentation of the benzyl radical, $C_6H_5CH_2$, $\tilde{X}\ ^2B_1$. The original mechanism[8] provided pathways for H atom loss and formation of the fulvenallenyl radical, C_5H_4—C≡CH. This suggestion also implies formation of the cyclopentadienyl radical and acetylene. The bicyclic radicals and vinylidene (:C=CH_2) will not be stable in the hot micro-reactor and are enclosed in brackets. The tropyl radical, C_7H_7, $\tilde{X}\ ^2E_2''$, does not participate.

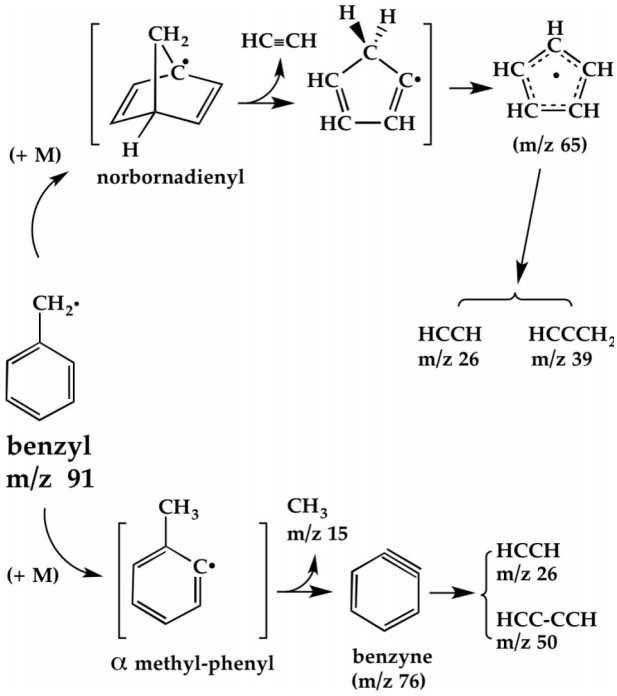

FIG. 14. Fragmentation pathways of the benzyl radical, $C_6H_5CH_2$, $\tilde{X}\ ^2B_1$, are shown. The internal H-atom abstraction from the ring that leads to the formation of the α methyl-phenyl radical will be endothermic[72] by roughly 1 eV. This process also requires a curve-crossing from the $^2B_1$ benzyl (π radical) to the $^2A'$ methyl-phenyl (σ radical). Decomposition of the α methyl-phenyl radical produces CH_3 and *o*-C_6H_4. A second pathway is the isomerization of benzyl to the bridgehead norbornadienyl radical. The α methyl-phenyl radicals, bridgehead norbornadienyl radicals, and $^2A'$ cyclopentadienyl radicals will not be stable in the hot micro-reactor and are enclosed in brackets. The tropyl radical, C_7H_7, $\tilde{X}\ ^2E_2''$, does not participate.

for thermal cracking of benzyl radicals that address these products.

The pyrolysis of $C_6H_5{}^{13}CH_2$ produces[7] both $^{13}CH_3$ (m/z 16) and *o*-C_6H_4 (m/z 76). These products could be the result of an isomerization of the ^{13}[benzyl] radicals to the [α ^{13}methyl-phenyl] radicals in Fig. 14. The isomerization would be initiated by H-abstraction from the aromatic ring by the —CH_2 side chain. Such an abstraction would be difficult because of a required ($\pi \rightarrow \sigma$) curve-crossing ($C_6H_5CH_2$, $^2B_1 \rightarrow C_6H_4CH_3$, $^2A'$). In addition the internal abstraction will be endothermic by about 1 eV because of the difference in the $C_6H_5CH_2$—H and C_6H_5—H bond energies (see Table I). Formation of the $C_6H_4CH_3$, $^2A'$ radical in Fig. 14 will be followed by rapid fragmentation to the methyl and *o*-benzyne radicals and both are confirmed to be present.[65] Heating *o*-C_6H_4 to high temperatures is known[66] to trigger fragmentation to HC≡CH and HC≡C—C≡CH. The pyrolysis reactions of both the $C_6H_5CD_2$ and $C_6D_5CH_2$ radicals are consistent with this pathway.[7] Decomposition of $C_6H_5CD_2$ radicals at 1500 K forms small quantities of the CD_2H (m/z 17) radicals while heating $C_6D_5CH_2$ radicals to 1400 K leads to appearance of CH_2D (m/z 16) radicals.

A second pathway for fragmentation of the benzyl radical shown in Fig. 14 is isomerization of $C_6H_5CH_2$ to the bridgehead, norbornadienyl radical. Such a bridgehead radical would suffer a retro-Diels-Alder fragmentation producing HC≡CH and the $^2A'$ C_5H_5 radical. The planar (σ) $^2A'$ C_5H_5

radical is certainly the initial adduct in the reaction[67,68] of propargyl with acetylene and it rapidly isomerizes to the ground state, cyclopentadienyl radical, C_5H_5, $\tilde{X}\ ^2E_1''$. The ^{13}[norbornadienyl] radical will automatically incorporate the ^{13}C label into the cyclopentadienyl radical, as observed in Fig. 13 of Ref. 7.

The pyrolysis pathways for $C_6H_5CH_2$ shown in Figs. 13 and 14 are consistent with all of the major peaks of the PIMS in Fig. 2 of Ref. 7. The corresponding pathways for the isotopically substituted benzyl radicals, $C_6H_5CD_2$, $C_6D_5CH_2$, and $C_6H_5{}^{13}CH_2$ are contained in Figs. S1–S6 in the supplementary material.[69] As in the case of the parent benzyl radical, these predicted $C_6H_5CD_2$, $C_6D_5CH_2$, and $C_6H_5{}^{13}CH_2$ pathways[69] can be used to assign the major peaks of the experimental PIMS spectra in Figs. 8, 10, and 11 of Ref. 7.

A recent paper[18] applied *metadynamics* to the pyrolysis of benzyl. These calculations suggested that both C_5H_5 and its isomer, $(CH_2)_2C—C{\equiv}CH$, are intermediates in the high temperature pyrolysis of benzyl. The IE(C_5H_5) is measured to be 8.4 eV (see Table I) and the measured[7] PIE(m/z 65) has its threshold at 8.4 ± 0.1 eV. The IE($HC{\equiv}C—C(CH_2)_2$) is not measured but it is likely less than that of the allyl radical, 8.1 eV (see Table I). The PIE(m/z 65) resulting from the thermal cracking of the $C_6H_5CH_2$ radical indicates that there is little (or no) $(CH_2)_2C—C{\equiv}CH$ present in the pyrolysis of benzyl. It was also predicted by the *metadynamics* calculations[18] that the initial $C_6H_5CH_2$ radicals could isomerize to a pair of isomeric, dimethylene-cyclopentenyl radicals. The spectroscopic probes of Ref. 7 could not confirm the presence of these two isomers.

There are small features at m/z 41, 51, 64, 77, and 78 present in the PIMS of $C_6H_5CH_2$ (Fig. 2 of Ref. 7) that cannot be rationalized by either pathways of Figs. 13 and 14. The peaks at m/z 77 and 78 are likely the phenyl radical (C_6H_5) and benzene. There is a theoretical calculation that predicts[64] a small channel for pyrolysis of fulvenallene to (C_5H_4: + $HC{\equiv}CH$). The singlet carbene (C_5H_4) is consistent with the peak at m/z 64.

There are small bands in the 118.2 nm PIMS spectra of $C_6H_5CD_2$ and $C_6D_5CH_2$ (Figs. 8 and 10 of Ref. 7) that suggest an interesting subtlety to the α methyl-phenyl radical in Fig. 14. Perhaps there is some equilibration of benzyl radicals with the α methyl-phenyl radicals? If so, then the $C_6H_5CD_2$ and $C_6D_5CH_2$ radicals will scramble: $C_6H_5CD_2 \leftrightharpoons [C_6H_4—CHD_2] \leftrightharpoons C_6H_4D—CHD$. Application of the [Benson fragmentation, methyl-phenyl, norbornadienyl] pathways to the *o*-$C_6H_4D—CHD$ radical leads to the formation of complex set of labeled (fulvenallenes, ethynl cyclpentadienes, and fulvenallenyl) radicals.[37] Fragmentation of these radicals predicts formation of $C_5H_4—C{\equiv}CH$ (m/z 89), C_5H_4D (cyclopentadienyl radical-d_1, m/z 66), *o*-C_6H_3 D (*o*-benzyne, m/z 77), $HC{\equiv}C—CH—C{\equiv}CH$ (m/z 63), and $DC{\equiv}C—C{\equiv}CD$ (m/z 52). There are signals in Fig. 8 of Ref. 7 that are compatible with these radicals. A similar scrambling of benzyl radical-d_5 ($C_6D_5CH_2 \leftrightharpoons [C_6D_4—CDH_2] \leftrightharpoons C_6D_4H—CHD$) leads to production of $C_5H_3D—CCH$ (m/z 92), C_5D_4H (m/z 69), *o*-C_6D_3H (m/z 79), and ($DC{\equiv}C—C{\equiv}C—CD_2$ or $DC{\equiv}C—CD—C{\equiv}CD$) m/z 66. Weak features for all of these radicals are present in Fig. 10 of Ref. 7.

Examination of the isotopic spectra for pyrolysis of benzyl radical permits a rough estimation of the energetics of the three decomposition pathways for benzyl radical. It appears that two channels (Benson fragmentation and the bridgehead norbornadienyl radical) open at roughly the same reactor temperature. The methy-phenyl radical channel becomes active at slightly higher temperatures. The PIMS spectrum of $C_6H_5{}^{13}CH_2$ (Fig. 11 in Ref. 7) demonstrates that benzyl radical decomposition begins at 1300 K. The Benson fragmentation products ^{13}(fulvenallene, m/z 91) and ^{13}(fulvenallenyl, m/z 90) are both observed. The norbornadienyl pathway produces ^{13}(cyclopentadienyl, m/z 66) while the methyl-phenyl radical channel generates ^{13}(CH_3, m/z 16) and both species are also present. For the case of the $C_6H_5CD_2$ radical, Fig. 8 of Ref. 7, radical decomposition is underway at 1300 K and products of the Benson fragmentation (m/z 91, 92, and 90) are present as well as cyclopentadienyl-d_2 (m/z 67) resulting from the norbornadienyl channel. Products from the methyl-phenyl radical channel, CHD_2 (m/z 17) and *o*-C_6H_4 (m/z 76), appear at 1500 K. Decomposition of the $C_6D_5CH_2$ radical (Fig. 10 of Ref. 7) yields a similar result; radicals from the methyl-phenyl radical channel, CDH_2 (m/z 16) and *o*-C_6D_4 (m/z 80), are detected at 1500 K. At 1300 K evidence of the Benson fragmentation (m/z 94, 95, 93) and the norbornadienyl route (cyclopentadienyl radical-d_3, m/z 68) is evident. Qualitatively it appears that the Benson fragmentation and the norbornadieneyl channels become activated at 1300 K while the methyl-phenyl radical pathway is present at 1500 K.

In principle it is possible to use the experimental results of the micro-reactor from this paper and Ref. 7 to put some bounds on the pyrolysis kinetics of the benzyl radical. As summarized in Figs. 13 and 14, there are at least three thermal decomposition pathways for the $C_6H_5CH_2$ radical. These are represented by Eqs. (6)–(8),

$$C_6H_5CH_2 \rightarrow C_5H_4—CCH_2 + H \rightarrow C_5H_4—C^{\circ}CH + H, \quad (6)$$

$$C_6H_5CH_2 \rightarrow [C_6H_4CH_3] \rightarrow CH_3 + C_6H_4, \quad (7)$$

$$C_6H_5CH_2 \rightarrow [\text{bridgehead norbornadienyl radical}] \rightarrow HC^{\circ}CH + C_5H_5. \quad (8)$$

If the residence time in the micro-reactor is roughly 0.1 ms, then reactions with a rate of less than 10^3 s^{-1} will not be observed while reactions with rates greater that 10^5 s^{-1} will appear to be complete. The *effective* transit time (i.e., residence in the "sweet spot") is even shorter, which puts a lower limit on the rate coefficients of the processes that can be observed. If kinetic modeling can provide a set of pre-exponential factors for Eqs. (6)–(8) or other reactions, then the residence time and the reactor temperature will put a bound on the heights of the barriers that this experiment can detect. Such estimates will require detailed computational fluid dynamics modeling of the SiC micro-reactor to find realistic residence times as well as the gas pressures and temperatures. This is an intriguing notion but is beyond the scope of this paper.

The decomposition of benzyl radical with its three distinct pyrolysis pathways (shown in Figs. 13 and 14) is

complicated. Nevertheless, the proposed mechanisms offer a set of predictions for the thermal cracking of more complex aromatic compounds that are included in surrogate fuel mixtures. Aviation fuels are composed of mixtures of a very large number of chemical components.[70] The detailed numerical simulation of real combustion fuels is currently too difficult to apply to any fuel that is not a pure component or a mixture of only a few species. One way to circumvent this problem is to study surrogate fuels. Such surrogate fuels should be comprised of a handful of components but be capable of emulating the gas phase combustion characteristics of the real fuel of interest. The advantage, of course, is that the resulting reaction mechanism will be a much more manageable size. A surrogate fuel for aviation diesels has been proposed[70] that is a mixture of ten compounds. This mixture includes 6 alkanes (*n*-decane, *n*-dodecane, iso-octane, iso-cetane, methyl cyclohexane, and n-butyl cyclohexane) and 4 aromatic species (toluene, *n*-propyl benzene,1,3,5-trimethyl benzene, and 1-methyl naphthalene). Three of these species (C_6H_5—CH_3, $C_6H_3(CH_3)_3$, and C_6H_5—$CH_2CH_2H_3$) would be predicted to pyrolyze to benzyl radicals. The decomposition pathways for $C_6H_5CH_2$ in Figs. 13 and 14 will be relevant to these surrogates.

ACKNOWLEDGMENTS

We congratulate Professor Dr. Jürgen Troe on his appointment as the Benson Lecturer at the 24th *International Symposium on Gas Kinetics and Related Phenomena*, July 2016. The authors gratefully acknowledge the extensive helpful discussions with Nicole Labbe, Raghu Sivaramakrishnan, Hans-Heinrich Carstensen, John D. Savee, Veronica M. Bierbaum, and John F. Stanton. We are also in the debt of an anonymous referee for several useful suggestions. We acknowledge support from the National Science Foundation (Grant Nos. CHE-1112466 and CBET-1403979) to J.P.P., G.T.B., J.W.D., and G.B.E. G.T.B. was also funded by the Marion L. Sharrah Memorial Fund at the University of Colorado. M.A., O.K., and T.P.T. and the Advanced Light Source are supported by the Director, Office of Energy Research, Office of Basic Energy Sciences, and Chemical Sciences Division of the U.S. Department of Energy under Contract No. DE-AC02- 05CH11231. D.J.R. and M.R.N. are supported by United States Department of Energy's Bioenergy Technology Office, under Contract No. DE-AC36-99GO10337 with the Sciences Division of the U.S. Department of Energy under Contract No. DE-AC02-05CH11231.

[1]M. B. Colket and D. J. Seery, "Reaction mechanisms for toluene pyrolysis," Symp. (Int.) Combust. **25**, 883–891 (1994).
[2]J. L. Burger, T. M. Lovestead, and T. J. Bruno, "Composition of the C_6+ fraction of natural gas by multiple porous layer open tubular capillaries maintained at low temperatures," Energy Fuels **30**, 2119–2126 (2016).
[3]J. L. Burger, M. E. Harries, and T. J. Bruno, "Characterization of four diesel fuel surrogates by the advanced distillation curve method," Energy Fuels **30**, 2813 (2016).
[4]C. J. Mueller, W. J. Cannella, T. J. Bruno, B. Bunting, H. D. Dettman, J. A. Franz, M. L. Huber, M. Natarajan, W. J. Pitz, M. A. Ratcliff, and K. Wright, "Methodology for formulating diesel surrogate fuels with accurate compositional, ignition-quality, and volatility characteristics," Energy Fuels **26**, 3284–3303 (2012).
[5]B. Shukla, A. Susa, A. Miyoshi, and M. Koshi, "*In situ* direct sampling mass spectrometric study on formation of polycyclic aromatic hydrocarbons in toluene pyrolysis," J. Phys. Chem. A **111**, 8308–8324 (2007).
[6]T. Zhang, L. Zhang, X. Hong, K. Zhang, F. Qi, C. K. Law, T. Ye, P. Zhao, and Y. Chen, "An experimental and theoretical study of toluene pyrolysis with tunable synchrotron VUV photoionization and molecular-beam mass spectrometry," Combust. Flame **156**, 2071–2083 (2009).
[7]G. T. Buckingham, T. K. Ormond, J. P. Porterfield, P. Hemberger, O. Kostko, M. Ahmed, D. J. Robichaud, M. R. Nimlos, J. W. Daily, and G. B. Ellison, "The thermal decomposition of the benzyl radical in a heated micro-reactor. I. Experimental findings," J. Chem. Phys. **142**, 044307–044320 (2015).
[8]V. S. Rao and G. B. Skinner, "Formation of hydrogen atoms in pyrolysis of ethylbenzene behind shock waves. Rate constants for the thermal dissociation of the benzyl radical," Proc. Combust. Inst. **21**, 809–814 (1986).
[9]R. D. Johnson, "Excited electronic states of the tropyl (cyclo-C_7H_7) radical," J. Chem. Phys. **95**, 7108–7113 (1991).
[10]T. Pino, F. Guthe, H. Ding, and J. P. Maier, "Gas-phase electronic spectrum of the tropyl C_7H_7 radical," J. Phys. Chem. A **106**, 10022–10026 (2002).
[11]V. L. Stakhursky, I. Sioutis, G. Tarczay, and T. A. Miller, "Computational investigation of the Jahn-Teller effect in the ground and excited electronic states of the tropyl radical. Part I. Theoretical calculation of spectroscopically observable parameters," J. Chem. Phys. **128**, 084310–084323 (2008).
[12]I. Sioutis, V. L. Stakhursky, G. Tarczay, and T. A. Miller, "Experimental investigation of the Jahn-Teller effect in the ground and excited electronic states of the tropyl radical. Part II. Vibrational analysis of the A $^2E_3''$–x $^2E_2''$ electronic transition," J. Chem. Phys. **128**, 084311–084329 (2008).
[13]R. Sivaramakrishnan, M. C. Su, and J. V. Michael, "H- and D-atom formation from the pyrolysis of $C_6H_5CH_2Br$ and $C_6H_5CD_2Br$: Implications for high-temperature benzyl decomposition," Proc. Combust. Inst. **33**, 243–250 (2011).
[14]J. Jones, G. B. Bacskay, and J. C. Mackie, "Decomposition of the benzyl radical: Quantum chemical and experimental (shock tube) investigations of reaction pathways," J. Phys. Chem. A **101**, 7105–7113 (1997).
[15]R. G. Satink, G. Meijer, and G. von Helden, "Infrared spectroscopy of neutral C_7H_7 isomers: Benzyl and tropyl," J. Am. Chem. Soc. **125**, 15714–15715 (2003).
[16]C. Cavallotti, M. Derudi, and R. Rota, "On the mechanism of decomposition of the benzyl radical," Proc. Combust. Inst. **32**, 115–121 (2009).
[17]M. Derudi, D. Polino, and C. Cavallotti, "Toluene and benzyl decomposition mechanisms: Elementary reactions and kinetic simulations," Phys. Chem. Chem. Phys. **13**, 21308–21318 (2011).
[18]D. Polino and M. Parrinello, "Combustion chemistry via metadynamics: Benzyl decomposition revisited," J. Phys. Chem. A **119**, 978–989 (2015).
[19]K. H. Fischer, P. Hemberger, A. Bodi, and I. Fischer, "Photoionisation of the tropyl radical," Beilstein J. Org. Chem. **9**, 681–688 (2013).
[20]Q. Guan, K. N. Urness, T. K. Ormond, D. E. David, G. B. Ellison, and J. W. Daily, "The properties of a micro-reactor for the study of the unimolecular decomposition of large molecules," Int. Rev. Phys. Chem. **33**, 447–487 (2014).
[21]M. Kaufmann, B. M. Broderick, and G. E. Douberly, "Helium nanodroplet infrared spectroscopy of the tropyl radical," in *70th International Symposium on Molecular Spectroscopy*, 2015.
[22]X. Zhang, A. V. Friderichsen, S. Nandi, G. B. Ellison, D. E. David, J. T. McKinnon, T. G. Lindeman, D. C. Dayton, and M. R. Nimlos, "Intense, hyperthermal source of organic radicals for matrix-isolation spectroscopy," Rev. Sci. Inst. **74**, 3077–3086 (2003).
[23]N. P. Lockyer and J. C. Vickerman, "Single photon ionisation mass spectrometry using laser-generated vacuum ultraviolet photons," Laser Chem. **17**, 139–159 (1997).
[24]J. Boyle and L. Pfefferle, "Study of higher hydrocarbon production during ethylacetylene pyrolysis using laser-generated vacuum-ultraviolet photoionization detection," J. Phys. Chem. **94**, 3336–3340 (1990).
[25]R. E. Bandy, C. Lakshminarayan, R. K. Frost, and T. S. Zwier, "The ultraviolet photochemistry of diacetylene—Direct detection of primary products of the metastable $C_4H_2^*$ + C_4H_2 reaction," J. Chem. Phys. **98**, 5362–5374 (1993).
[26]P. A. Heimann, M. Koike, C. W. Hsu, D. Blank, X. M. Yang, A. G. Suits, Y. T. Lee, M. Evans, C. Y. Ng, C. Flaim, and H. A. Padmore, "Performance of the vacuum ultraviolet high-resolution and high-flux beamline for chemical dynamics studies at the advanced light source," Rev. Sci. Inst. **68**, 1945–1951 (1997).
[27]A. Vasiliou, K. M. Piech, X. Zhang, M. R. Nimlos, M. Ahmed, A. Golan, O. Kostko, D. L. Osborn, J. W. Daily, J. F. Stanton, and G. B. Ellison, "The products of the thermal decomposition of CH_3CHO," J. Chem. Phys. **135**, 14306–14311 (2011).

[28]T. K. Ormond, A. M. Scheer, M. R. Nimlos, D. J. Robichaud, J. W. Daily, J. F. Stanton, and G. B. Ellison, "Polarized matrix infrared spectra of cyclopentadienone: Observations, calculations, and assignment for an important intermediate in combustion and biomass pyrolysis," J. Phys. Chem. A **118**, 708–718 (2014).
[29]F. A. Elder and A. C. Parr, "Photoionization of the cycloheptatrienyl radical," J. Chem. Phys. **50**, 1027–1028 (1969).
[30]J. C. Traeger and R. G. McLoughlin, "Threshold photoionization and dissociation of toluene and cycloheptatriene," J. Am. Chem. Soc. **99**, 7351–7352 (1977).
[31]A. K. Vasiliou, K. M. Piech, B. Reed, X. Zhang, M. R. Nimlos, M. Ahmed, A. Golan, O. Kostko, D. L. Osborn, K. N. Urness, D. E. David, J. W. Daily, J. F. Stanton, and G. B. Ellison, "Thermal decomposition of CH_3CHO studied by matrix infrared spectroscopy and photoionization mass spectroscopy," J. Chem. Phys. **137**, 164308 (2012).
[32]K. N. Urness, Q. Guan, A. Golan, J. W. Daily, M. R. Nimlos, J. F. Stanton, M. Ahmed, and G. B. Ellison, "Pyrolysis of furan in a microreactor," J. Chem. Phys. **139**, 124305–124314 (2013).
[33]A. M. Scheer, C. Mukarakate, D. J. Robichaud, G. B. Ellison, and M. R. Nimlos, "Radical chemistry in the thermal decomposition of anisole and deuterated anisoles: An investigation of aromatic growth," J. Phys. Chem. A **114**, 9043–9056 (2010).
[34]L. V. Moskaleva and M. C. Lin, "Unimolecular isomerization/decomposition of cyclopentadienyl and related bimolecular reverse process: *Ab initio* MO/statistical theory study," J. Comput. Chem. **21**, 415–425 (2000).
[35]H. J. Wörner and F. Merkt, "Diradicals, antiaromaticity, and the pseudo-Jahn-Teller effect: Electronic and rovibronic structures of the cyclopentadienyl cation," J. Chem. Phys. **127**, 034303–034319 (2007).
[36]J. D. Savee, personal communication (2014).
[37]G. T. Buckingham, *Pyrolysis and Spectroscopy of Cyclic Aromatic Combustion Intermediates* (University of Colorado, 2016).
[38]H. Gao, Y. T. Xu, L. Yang, C. S. Lam, H. L. Wang, J. A. Zhou, and C. Y. Ng, "High-resolution threshold photoelectron study of the propargyl radical by the vacuum ultraviolet laser velocity-map imaging method," J. Chem. Phys. **135**, 224304–224311 (2011).
[39]J. D. Savee, S. Soorkia, O. Welz, T. M. Selby, C. A. Taatjes, and D. L. Osborn, "Absolute photoionization cross-section of the propargyl radical," J. Chem. Phys. **136**, 134307–134317 (2012).
[40]S. H. Luu, K. Glanzer, and J. Troe, "Thermal isomerization in shock-waves and flash-photolysis of cycloheptatriene. III," Ber. Bunsenges. Phys. Chem. **79**, 855–858 (1975).
[41]W. C. Herndon and L. L. Lowry, "Mechanism of pyrolysis of bicyclo [2.2.1] heptadiene. Kinetics of bicyclo [2.2.1] heptadiene to toluene isomerization," J. Am. Chem. Soc. **86**, 1922–1926 (1964).
[42]R. Sustmann, D. Brandes, F. Lange, and U. Nuchter, "Rearrangements of free-radicals.11. sigmatropic and electrocyclic reactions of bicyclo [3.2.0] heptadienyl radicals, 3-quadricyclanyl radicals, and 7-norbornadienyl radical," Chem. Ber. **118**, 3500–3512 (1985).
[43]C. Cavallotti, S. Mancarella, R. Rota, and S. Carra, "Conversion of C_5 into C_6 cyclic species through the formation of C_7 intermediates," J. Phys. Chem. A **111**, 3959–3969 (2007).
[44]N. Fuson, C. Garrigoulagrange, and M. L. Josien, "Spectre infrarouge et attribution des vibrations des toluenes $C_6H_5CH_3$, $C_6H_5CD_3$ et $C_6D_5CD_3$," Spectrochim. Acta **16**, 106–127 (1960).
[45]E. G. Baskir, A. K. Maltsev, V. A. Korolev, V. N. Khabashesku, and O. M. Nefedov, "Generation and IR spectroscopic study of benzyl radical," Russ. Chem. Bull. **42**, 1438–1440 (1993).
[46]A. M. Scheer, C. Mukarakate, D. J. Robichaud, M. R. Nimlos, H.-H. Carstensen, and G. B. Ellison, "Unimolecular thermal decomposition of phenol and d_5-phenol: Direct observation of cyclopentadiene formation via cyclohexadienone," J. Chem. Phys. **136**, 044309–044320 (2012).
[47]J. D. Savee, T. M. Selby, O. Welz, C. A. Taatjes, and D. L. Osborn, "Time- and isomer-resolved measurements of sequential addition of acetylene to the propargyl radical," J. Phys. Chem. Lett. **6**, 4153–4158 (2015).
[48]D. C. Astholz and J. Troe, "Thermal-decomposition of benzyl radicals in shock-waves," J. Chem. Soc., Faraday Trans. 2 **78**, 1413–1421 (1982).
[49]L. Brouwer, W. Müller-Markgraf, and J. Troe, "Thermal-decomposition of ethylbenzene in shock-waves," Ber. Bunsenges. Phys. Chem. **87**, 1031–1036 (1983).
[50]L. D. Brouwer, W. Müller-Markgraf, and J. Troe, "Thermal-decomposition of toluene—A comparison of thermal and laser-photochemical activation experiments," J. Phys. Chem. **92**, 4905–4914 (1988).
[51]R. Fröchtenicht, H. Hippler, J. Troe, and J. P. Toennies, "Photon-induced unimolecular decay of the benzyl radical—1st direct identification of the reaction pathway to C_7H_6," J. Photochem. Photobiol., A **80**, 33–37 (1994).
[52]W. Müller-Markgraf and J. Troe, "Thermal decomposition of benzyl iodide and of benzyl radicals in shock waves," J. Phys. Chem. **92**, 4899–4905 (1988).
[53]M. A. Oehlschlaeger, D. F. Davidson, and R. K. Hanson, "High-temperature thermal decomposition of benzyl radicals," J. Phys. Chem. A **110**, 6649–6653 (2006).
[54]K. M. Pamidimukkala, R. D. Kern, M. R. Patel, H. C. Wei, and J. H. Kiefer, "High-temperature pyrolysis of toluene," J. Phys. Chem. **91**, 2148–2154 (1987).
[55]A. Alexiou and A. Williams, "soot formation in shock-tube pyrolysis of toluene, toluene-methanol, toluene-ethanol, and toluene-oxygen mixtures," Combust. Flame **104**, 51–65 (1996).
[56]P. Dagaut, G. Pengloan, and A. Ristori, "Oxidation, ignition and combustion of toluene: Experimental and detailed chemical kinetic modeling," Phys. Chem. Chem. Phys. **4**, 1846–1854 (2002).
[57]P. Dagaut, A. Ristori, A. El Bakali, and M. Cathonnet, "Experimental and kinetic modeling study of the oxidation of n-propylbenzene," Fuel **81**, 173–184 (2002).
[58]R. Sivaramakrishnan, R. S. Tranter, and K. Brezinsky, "High pressure pyrolysis of toluene. 1. Experiments and modeling of toluene decomposition," J. Phys. Chem. A **110**, 9388–9399 (2006).
[59]M. Shapero, N. C. Cole-Filipiak, C. Haibach-Morris, and D. M. Neumark, "Benzyl radical photodissociation dynamics at 248 nm," J. Phys. Chem. A **119**, 12349–12356 (2015).
[60]G. Porter and M. I. Savadatt, "Electronic spectra of benzyl—A new transition," Spectrochim. Acta **22**, 803–806 (1966).
[61]A. H. Laufer, "An excited-state of acetylene—Photochemical and spectroscopic evidence," J. Chem. Phys. **73**, 49–52 (1980).
[62]K. M. Ervin, J. Ho, and W. C. Lineberger, "A study of the singlet and triplet-states of vinylidene by photoelectron-spectroscopy of $H_2C{=}C^-$, $D_2C{=}C^-$, and $HDC{=}C^-$—Vinylidene acetylene isomerization," J. Chem. Phys. **91**, 5974–5992 (1989).
[63]G. da Silva, A. J. Trevitt, M. Steinbauer, and P. Hemberger, "Pyrolysis of fulvenallene (C_7H_6) and fulvenallenyl (C_7H_5): Theoretical kinetics and experimental product detection," Chem. Phys. Lett. **517**, 144–148 (2011).
[64]D. Polino and C. Cavallotti, "Fulvenallene decomposition kinetics," J. Phys. Chem. A **115**, 10281–10289 (2011).
[65]It could be possible for the α methyl-phenyl radical, α C_6H_4—CH_3, to form the α methylbenzyne, α C_6H_3—CH_3 by H atom loss. However a scan of the PIE (m/z 90) identifies m/z 90 as fulvenallene, $C_5H_4{=}C{=}CH_2$. There is no evidence for the presence of α C_6H_3—CH_3.
[66]X. Zhang, A. T. Maccarone, M. R. Nimlos, S. Kato, V. M. Bierbaum, G. B. Ellison, B. Ruscic, A. C. Simmonett, W. D. Allen, and H. F. Schaefer, "Unimolecular thermal fragmentation of *ortho*-benzyne," J. Chem. Phys. **126**, 044312–044322 (2007).
[67]V. D. Knyazev and I. R. Slagle, "Kinetics of the reaction between propargyl radical and acetylene," J. Phys. Chem. A **106**, 5613–5617 (2002).
[68]J. D. Savee, J. Zador, P. Hemberger, B. Sztaray, A. Bodi, and D. L. Osborn, "Threshold photoelectron spectrum of the benzyl radical," Mol. Phys. **113**, 2217–2227 (2015).
[69]See supplementary material at http://dx.doi.org/10.1063/1.4954895 for the pyrolysis pathways for the $C_6H_5CD_2$, $C_6D_5CH_2$, and $C_6H_5{}^{13}CH_2$ radicals.
[70]S. Dooley, S. H. Won, M. Chaos, J. Heyne, Y. Ju, F. L. Dryer, K. Kumar, C.-J. Sung, H. Wang, M. A. Oehlschlaeger, R. J. Santoro, and T. A. Litzinger, "A jet fuel surrogate formulated by real fuel properties," Combust. Flame **157**, 2333–2339 (2010).
[71]J. B. Pedley, R. D. Naylor, and S. P. Kirby, *Thermochemistry of Organic Compounds*, 2nd ed. (Chapman and Hall, New York, 1986).
[72]S. J. Blanksby and G. B. Ellison, "Bond dissociation energies of organic molecules," Acc. Chem. Res. **36**, 255–263 (2003).
[73]T. Ichino, S. W. Wren, K. M. Vogelhuber, A. J. Gianola, W. C. Lineberger, and J. F. Stanton, "The vibronic level structure of the cyclopentadienyl radical," J. Chem. Phys. **129**, 084310 (2008).
[74]J. A. Blush, P. Chen, R. T. Wiedmann, and M. G. White, "Rotationally resolved threshold photoelectron-spectrum of the methyl radical," J. Chem. Phys. **98**, 3557–3559 (1993).
[75]S. T. Pratt, P. M. Dehmer, and J. L. Dehmer, "Zero-kinetic-energy photoelectron-spectroscopy from the $\tilde{a}\ ^1A_u$ state of acetylene—Renner-Teller interactions in the *trans*-bending vibration of $C_2H_2{}^+\,X\,^2\prod_u$," J. Chem. Phys. **99**, 6233–6244 (1993).

[76]X. Xing, B. Reed, K. C. Lau, C. Y. Ng, X. Zhang, and G. B. Ellison, "Vacuum ultraviolet laser pulsed field ionization-photoelectron study of allyl radical CH_2CHCH_2," J. Chem. Phys. **126**, 171170–171174 (2007).
[77]F. A. Houle and J. L. Beauchamp, "Detection and investigation of allyl and benzyl radicals by photoelectron-spectroscopy," J. Am. Chem. Soc. **100**, 3290–3294 (1978).
[78]X. Zhang and P. Chen, "Photoelectron-spectrum of *o*-benzyne—Ionization-potentials as a measure of singlet triplet gaps," J. Am. Chem. Soc. **114**, 3147–3148 (1992).
[79]M. Steinbauer, P. Hemberger, I. Fischer, and A. Bodi, "Photoionization of C_7H_6 and C_7H_5: Observation of the fulvenallenyl radical," ChemPhysChem **12**, 1795–1797 (2011).
[80]G. C. Eiden, F. Weinhold, and J. C. Weisshaar, "Photoelectron-spectroscopy of free-radicals with cm^{-1} resolution—The benzyl cation," J. Chem. Phys. **95**, 8665–8668 (1991).
[81]K. T. Lu, G. C. Eiden, and J. C. Weisshaar, "Toluene cation—Nearly free rotation of the methyl-group," J. Phys. Chem. **96**, 9742–9748 (1992).
[82]J. C. Traeger and R. G. McLoughlin, "Photo-ionization study of energetics of $C_7H_7^+$ ion formed from C_7H_8 precursors," Int. J. Mass Spectrom. Ion Phys. **27**, 319–333 (1978).
[83]T. Shimanouchi, *Tables of Vibrational Frequencies, Consolidated Vol. I*, NSRDS-NBS Vol. 39, p. 1972. The IR active modes of acetylene in an Ar matrix are slightly shifted from their gas-phase values. For the case of HC≡CH the Ar matrix frequences are $\sigma_u\ \nu_3 = 3302\ cm^{-1}$ and $3288\ cm^{-1}$ (splitting by the Darling-Dennison resonance is $14\ cm^{-1}$ in the cryogenic matrix) and the $\pi_u\ \nu_5$ is $736.8\ cm^{-1}$. For DC≡CD the matrix frequencies are $\sigma_u\ \nu_3 = 2442\ cm^{-1}$ and $\pi_u\ \nu_5$ is $736.8\ cm^{-1}$. The symmetry is broken in acetylene-d_1, HC≡CD. The matrix frequencies are $\sigma^+\ \nu_1 = 3340\ cm^{-1}$, $\sigma^+\ \nu_2 = 1854\ cm^{-1}$, $\sigma^+\ \nu_3 = 2586\ cm^{-1}$, $\pi\ \nu_4 = 518\ cm^{-1}$, and $\pi\ \nu_5 = 683\ cm^{-1}$.